Field Mapping of Large Aperture Superconducting Quadrupoles

P. Vernin and J. Le Bars
CEA/DAPNIA, C.E. Saclay, France

H. Fonvieille and G. Quéméner
LPCCF IN2P3–CNRS, Université Blaise Pascal, Clermont-Ferrand, France

J. Billan
CERN, Geneva, Switzerland

***Abstract* —The three quadrupoles of a High Resolution Spectrometer (Jefferson Lab., hall A) were mapped using an array of 10 coils of well defined geometry. The Q1 quadrupole has a 30 cm diameter bore and was measured over 1.6 m. The dimensions for Q2 and Q3 are 60 cm and 3.2 m. The results for Q1 are compared to an integral coil measurement. Detailed maps are extracted using a 3D harmonics analysis and the reference to filament models of the quadrupoles. The typical accuracy achieved is 0.1 mm (in radius) and 1 Gauss in the mapping volume, for a maximum field of 1.25 Tesla.**

I Introduction

Jefferson Lab. (or Thomas Jefferson National Accelerator Facility) is a new research facility located at Newport News, Virginia, USA. Its main equipment is a superconducting electron accelerator, CEBAF (Continuous Electron Beam Facility), devoted to hadronic physics. A 4GeV and 200μA beam can be delivered in three experimental end stations: Hall A, Hall B and Hall C. Hall A is focused on high resolution and high luminosity electron scattering experiments in coincidence on proton and heavier nuclei. It is equipped with two large identical magnetic spectrometers called Electron HRS and Proton HRS (High Resolution Spectrometer) whose design momentum resolutions are a few 10^{-5}.

TABLE I . Main Characteristics of the Quadrupoles

	Q1	**Q2/Q3**
Clear bore	300 mm	600 mm
Magnetic length	948 mm	1800 mm
Field gradient	8.31 T/m	3.5 T/m
Gradient uniformity (integral)	10^{-3}	10^{-3}
Operating current	3250 A	1850 A

Each HRS is made of three superconducting quadrupoles and a superconducting dipole, which must be mapped with high field and position accuracy. The goal of the QMM project [1] (Quadrupole Magnetic Measurement, a collaboration between the DAPNIA Saclay and the IN2P3 Clermont Ferrand, France) was to map the six quadrupoles. The scope of this paper is to report on the mapping of the three quadrupoles, called Q1, Q2 and Q3, of the Electron HRS. These quadrupoles are of "$\cos(2\theta)$" and room temperature yokes types. Q1 is described in [2,3] and Q2/Q3 in [4]. The main characteristics of these magnets are given in Table I

Manuscript received October 20,1997.

G. Quéméner, present affiliation: Jefferson Lab., Newport News, Va. USA.

II Mapping Specifications

The mapping specifications are based on accuracy requirements on the determination of spectrometer optics and phase space acceptance [5]. We used ray tracing through idealized field distributions to measure the effect of small changes of the field on global properties of the spectrometers. The resulting specifications are more demanding than in the case of usual beam line magnets, where only the field integral must be measured. Due to the large bore/length ratio of the magnets, to the large acceptance of the spectrometer and to the strong curvature of the trajectories in the quadrupoles, a detailed space distribution of the three components of the field is needed here. The mapping specifications are:

— accuracy on field components: <5 Gauss,
— accuracy on the field measurement position:
  – axial position (along the trajectories): 1 mm,
  – transverse position: 0.1 mm,
— accuracy on quadrupole axis position: 0.1 mm,
— accuracy on quadrupole roll angle: 1 mradian,
— accuracy on field integral: 1 Tmm,
— mapping length: 1.6 m (Q1), 3.2 m (Q2/Q3),
— mapping diameter: 300 mm (Q1), 600 mm (Q2/Q3),
— minimum current: 0 A,
— maximum current: ±3250 A (Q1) ±1850 A (Q2/Q3).

According to these specifications, we decided to map the quadrupoles *in situ*, in order to include in our measurement the effects of the gravity (Q3 axis is at 45° from the horizontal), of the magnet to magnet fringing field interference and of the parasitic magnetization of the environment.

III Design of the Mapping Device

To meet these requirements, we adopted a design based on an array of rotating coils rather than Hall probes. Using high precision VFC (Voltage to Frequency Convertor) for signal processing, high resolution shaft encoder for angle control and in flight acquisition mode, rotating coils provide fast and accurate flux measurements. In addition, their calibration is based on a direct control of the geometry of the coils, which is much easier than usual 3D calibrations of Hall probes.

So the mapping device is a single rigid object, rotating around an axis and carrying the array of coils. The axis of rotation coincides with the axis of the quadrupole and the coils are of rectangular shape and radial type. The mapping length is covered by ten identical coils in such a way that a coil stops exactly where the next one starts. In the radial direction, the coil surface extends from the rotation axis ($r = 0$) up to a radius slightly smaller than the quadrupole clear radius. In the case of beam line magnets, the quantities of interest are usually small high order harmonics of the field, so it is necessary to buck the fundamental component of the field.

Here the quantity of interest is the field itself, dominated by the quadrupole term, and there is no need to use the bucking coil technique. A mapping device, called here "probe", was built for Q1, and an other for Q2/Q3.

IV Coil Design

The coil mandrel is a carefully machined and controlled part made of glass-epoxy. Its cross section is a rectangle with chamfers, on which the 100 μm diameter wire is wound. To meet the accuracy requirements we adopted:

— Cu-Be for wire material, as it can be wound at much higher tightness than pure Cu wire,
— single layer winding,
— a 20 μm thick space between turns.

The main characteristics of the coil are given in Table II.

TABLE II Characteristics of the Coils

	Q1 probe	Q2/Q3 probe
Number of coils	10	10
Inner radius	0 mm	0 mm
Outer radius *Rmax*	140 mm	280 mm
coil length (along the axis)	160 mm	320 mm
number of turns	180	100
coil magnetic area	4.032 m^2	8.960 m^2
Electrical resistance	540 Ω	600 Ω
bare wire diameter	100 μm	100 μm
insulated wire diameter	110 μm	110 μm
wire pitch	130 μm	130 μm

During the winding, the position of each individual wire on the mandrel was controlled by means of a microscope and a linear encoder. After winding, the coil was stopped by an impregnation spray. The magnetic area of each coil was measured at CERN in an homogenous dipole field. This measurement was in agreement, within 3 10^{-4} relative, with the area computed from the optical controls.

V Probe Structure

The role of the probe structure is to provide a rigid support to the array of coils. We adopted for both probes (Q1 probe and Q2/Q3 probe) the solution of a thin cylinder of large diameter made of composite materials. Compared to a "X" shaped cross-section of the same weight, the same diameter and made of the same material, the cylinder has a small advantage in term of bending rigidity (1:1.25) and a huge advantage in term of torsional rigidity (1:470). The material is made by winding fibers on a mandrel at different angles. In our most critical case (Q2/Q3 probe), we improved dramatically the bending rigidity by inserting a layer of Carbon fibers "wound" at 0° with respect to the axis, between each two layers of glass fiber wound at +60° and —60°. The Carbon fiber provides the bending rigidity and the glass fiber provides both the torsional rigidity and the necessary global electrical insulation of the material.

Two boards of glass epoxy/honey comb sandwiches are glued inside the cylinder, on either side of a diameter, exhibiting a "Θ" shaped cross section. The coils are fixed between these two boards. The radius of the cylinder is slightly smaller than the outer radius of the coil. So a small part of each coil juts out the structure through a rectangular aperture made in the cylinder.

Two shafts, carrying the inner part of ceramic ball bearings, are fixed on the ends of the cylinder. These shafts and the ten coils are glued with high relative position accuracy on the "Θ" shaped composite structure by means of a rigid and accurate assembly jig.

The rotating probe is mounted inside a fixed cylinder called "container", made of pure carbon fiber. The container has thin end caps made of aluminium alloy and holding the outer part of the ball bearings. It plays a role of support and protection of the probe. It fits inside the quadrupole bore with a few *mm* clearance, allowing the fine adjustment of the rotation axis of the probe on the quadrupole axis. A special attention was paid to the design of the ball bearing supports in order to minimize the play and the friction of the bearings.

VI Motor, Encoder and Transmission Shaft

A stepping motor (16 microsteps per step and 200 steps per turn) drives a shaft by means of a speed reducer (1:100) and a pair of pulleys (1:2). One end of this shaft drives the encoder (18 bits, incremental with turn index). The other end drives the probe. Due to local mapping conditions, the shaft linking the motor-encoder set and the probe is 3.5 m long. The motor-encoder set has its own independent support system. The 3.5 m long shaft is a cylinder of 150 mm diameter made of pure Carbon fiber. A special attention was paid to the design of the transmission shaft linking the probe to the encoder: a high torsional rigidity, no play and a large tolerance to misalignments between the motor-encoder set and the probe. A set of spirit levels, glued on the probe structure, provides a reference rotation angle with an accuracy of 100 μradian. The measurement is made over one turn of the probe (two turns when one includes the acceleration ramps) and the rotation period is 12 s.

VII Electronics and Acquisition

The computer is a SUN Sparc 5 UNIX workstation controlling the mapping device by means of C programs. It is connected to a VME crate through a "Sbus" interface and to other devices (analog multiplexer and motor control electronics) through RS232 interfaces. Inside the VME crate, two Metrolab's Precision Digital Integrators 5035 (PDI: programmable amplifier and VFC) boards perform the acquisition of the coil signals and encoder data. Each one of the two PDI boards can be connected to any of the 10 coils by means of two ten channels electronic analog multiplexers.

The acquisition of the full map at a given current includes ten single coil acquisitions: one per individual coil. A single coil acquisition includes two elementary acquisitions: one during the clockwise turn followed by one during the counter-clockwise turn. So the total number of elementary acquisitions is 20. One PDI channel is used to scan the ten coils (coil #1 to coil #10) while the second channel reads 20 times the same coil (coil #6, located in the central part of the magnet). This provides a way to normalize the 20 elementary acquisitions with reference to one of them, for example the first one (coil #6 associated with the forward acquisition of coil #1). This resulted in a significant accuracy improvement

for the mapping of one of the quadrupoles (Q3), as its power supply suffered a long term drift at high current.

VIII Geometrical Controls of the Probes

In this measurement the harmonic components of the field are dominated by the quadrupole term and the coil surface extends from $r = 0$ to $r = Rmax$. In these conditions the field measurement accuracy will be governed by our knowledge of the part of the coil located at $r = Rmax$: the actual value of $Rmax$ and the angular position of its symmetry axis with respect to a reference angle. This part of the coil, which is located outside the probe structure, was controlled by means of a theodolite. For each one of the 10 coils of both probes, two position errors were measured with an accuracy between 10 to 20 μm: the "*radial error*" , i.e. the difference between the actual value and the nominal value of $Rmax$, and the "*transverse error*" , i.e. the distance of the coil symmetry axis to an horizontal plane including the rotation axis, the probe angle being at its nominal "horizontal coil" value. By comparing two sets of measurements done at two probe angles different by 180°, we analyzed the *transverse error* itself in term of "*permanent transverse error*", independent of the gravity, and "*probe sag*", due to the gravity. Maximum values of positions errors and sags are given in Table III for the six central coils.

TABLE III Position Errors and Sags of Coils #3 to #8

	Q1 probe	**Q2/Q3 probe**
Radial error	< 100 μm	< 60 μm
Permanent transverse error	< 20 μm	< 50 μm
Sag (coil plan is horizontal)	< 20 μm	< 30 μm
Sag (coil plan is vertical)	< 10 μm	< 20 μm

IX On Line Data Analysis

The PDI data include the flux increment values (VFC read out), the probe angle values (encoder read out) and the measurement time for each trigger. 200 triggers are generated per turn of the probe (1.8° angle steps). At the end of the 20 elementary acquisitions, data are processed according to the following sequence:

- correct flux increments from coil electrical resistance,
- correct flux increments from electronic offset,
- reverse the order of backward data,
- integrate flux increments to get flux values,
- force average flux to be zero,
- compute flux harmonics up to order 24,
- based on the harmonic analysis, correct flux and angle data from:
  - probe phase shift, with reference to coil #6 data of the first elementary acquisition (see section VII),
  - coil radial position error,
  - coil finite thickness,
  - coil transverse position error,
  - coil sag,
  - global phase shift (force the integral skew quadrupole term to be zero),
  - drift of the power supply, with reference to coil #6 data of the first elementary acquisition (see section VII),
- average forward and backward flux data,
- normalize flux data to the operating current of the magnet,
- compute final flux harmonics,
- compute probe alignment errors with respect to the symmetry plans of the magnet,
- compute harmonics of the integral flux,
- compute harmonics of the integral field.

The control by the operator of this process is based on the graphic display of the data at each step of the process. The computations and corrections concerning the geometry of the coils are detailed in [6]. The data precessing will be given in details in [7]

X Off Line Data Analysis

Starting from the flux harmonics of each individual coil, the role of the off line analysis is to compute the detailed field map of the quadrupole. The problem comes from the fact that we do not have an infinite number of coils along the axis, but just 10 of them. In fact the quadrupole was "cut" in 10 slices of the same thickness, and our data are accurate measurements of the flux integral of each slice. To solve this problem we use a theoretical model of the field distribution as an interpolation function.

From CEBAF magnet specifications and manufacturer documents, we have a detailed description of the magnet's coil and yoke geometry. From these data we build a computer model of the magnet coil. This model is made of about 20,000 straight filaments in 3D space. In order to take into account the contribution of the yoke, we add to the first set of filaments a second set which is the mirror image of the magnet coil given by the inner surface of the yoke [8]. A filament model was built for Q1, an other for Q2/Q3. The field distribution is computed by performing the integration of the Biot-Savart law along the filaments of the final model. From the field distribution, the flux in the measurement coils is computed by performing a new integration. The effect of the coil's chamfers is introduced at this level (see Section IV). The flux is computed for all the coils and for the 200 angle steps of the measurement. At the end of this process, we get model flux which can be compared directly to the measured flux. For both magnets, both flux were in agreement within about 1% of the amplitude of the fundamental component.

Measured flux are then processed according to the following sequence (*z* is the coordinate measured along the axis of the quadrupole):

- the model flux are subtracted from the measures ones. The (small) result is called "residual flux",
- the residual flux is analyzed in term of integrals along *z* of Fourier-Bessel functions of *z* (extension to 3D of the 2D harmonic analysis, see [7,9])
- a fitting procedure is used to compute the Fourier-Bessel functions from their integral [7]; this step is an approximation which can be tolerated here as it concerns only a small part of the total flux,
- the "residual field map" is computed from the Fourier-Bessel functions,
- the "model field map" is computed from the filament model
- the final field map is then obtained by adding the "residual field map" and the "model field map".

XI RESULTS

It is not possible to give here the complete results. Nevertheless some partial results are given in Fig. 1, 2 and 3.

Fig. 1 concerns the integral results of Q1, plotted in the (Normal × Skew) plan. The harmonics from *nh*=1 (dipole) to *nh*=10 and *nh*=14, given at the reference radius (150 mm), are plotted. Note that the dipole term is forced to zero by the alignment procedure. These integral results were found to be in agreement within 10^{-4} Tm with an integral measurement (using the bucking coil technique) performed at Saclay. In the case of the QMM measurement, the normal part of the sextupole (*nh*=3) term is very sensitive to the correction of the probe sag. The comparison with the bucked integral measurement was a severe test of the sag correction.

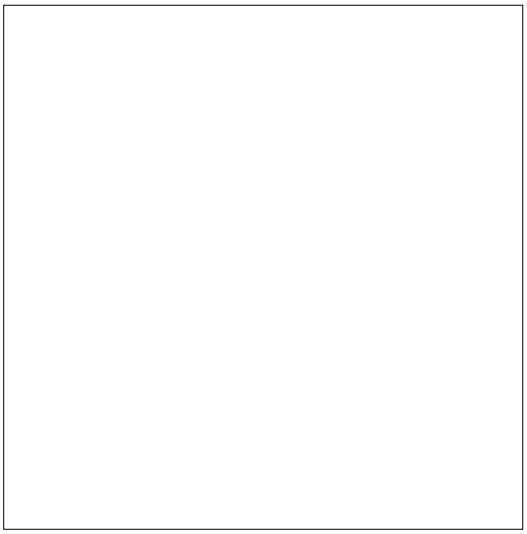

Fig. 1. Integral harmonics of Q1

Fig. 2 and 3 concerns the evolution along the axis of the quadrupole component (Fig.2) and the Dodecapole component (Fig. 3) of Q2 in term of field averaged over the coil length for 3 fields: the ideal (or model) field, the measured field and the residual field. In the case of the model and of the residual, the lineshape of the field is also plotted. The field is given at the reference radius (600 mm). Note the change in the vertical scale between the top and the bottom curves.

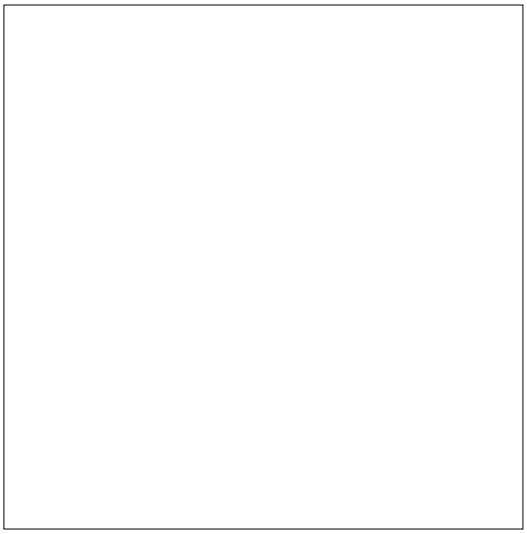

Fig. 2. Quadrupole term of Q2 as function of *z*

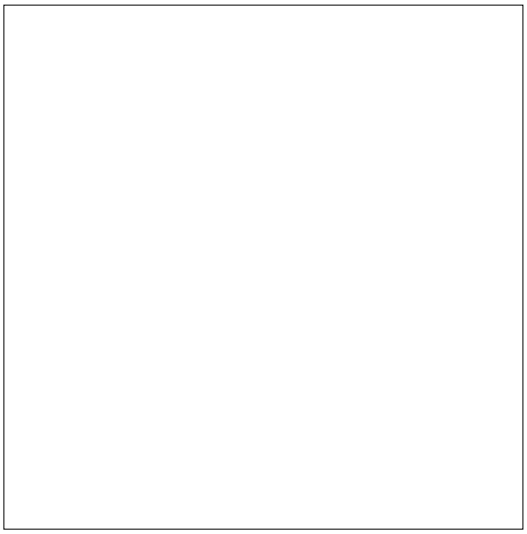

Fig. 3. Dodecapole term of Q2 as function of *z*

XII CONCLUSION

The detailed field distributions of the three quadrupoles of the Electron HRS were measured *in situ* with the required accuracy. This measurement allowed an accurate alignment of the quadrupoles with respect to the dipole and a precise determination of the optical properties and of the phase space acceptance of the spectrometer (work presently in progress). Concerning the Hadron HRS, Q1 was measured at Saclay (this measurement is reported in [10]). If it appears as necessary in order to understand discrepancies between the properties of the two spectrometers, Q2 and Q3 Hadron will be measured also.

REFERENCES

[1]H. Fonvieille et al., *QMM Project: A Proposal for Field Map Measurement of the six HRS Quadrupoles in Hall A, CEBAF*, LPCCF Report PCCI-RI 9415, 1994.

[2]A. Daël *et al., Design and Manufacturing of the Q1 Quadrupole for the CEBAF High Resolution Spectrometer,* IEEE Transaction on Magnetics, Vol. 30, n°4, pp. 2443-2446, July 1994.

[3]B. Gallet *et al., Test Results of the Q1 Quadrupoles for the CEBAF High Resolution Spectrometer,* IEEE Transaction on Magnetics, Vol. 32, n°4, pp. 2167-2170, July 1996.

[4]R. Kreutz, *Design of Superconducting Quadrupole Magnets for CEBAF's Hall A Spectrometer,* Proceedings of Particle Accelerator Conference, Washington, 1993.

[5]*CEBAF Conceptual Design Report, Basic Experimental equipment,* April 13, 1990 (Revised)

[6]H. Fonvieille et al., *Projet QMM: Calcul des Désalignements de la sonde en 2D*, LPCCF Report PCCI-RI 9608, 1996.

[7]G.Quéméner, Thèse, Clermont Ferrand, December 1997, to be published.

[8]K.-H. Meß, *Superconducting Accelerator Magnets,*Proceedings of the CERN Accelerator School, Superconductivity in Particle Accelerators, Hambourg 1988, p. 87.

[9]W.G. Davies, *The Theory of the Measurement of Magnetic Multipole Fields with Rotating Coil Magnetometers*, NIM A 311 (1992) pp. 339-436

[10]G. Quéméner, Proceeding of IMMW9, Saclay, 1995